RESEARCH ARTICLE
doi: 10.2306/scienceasia1513-1874.2023.029

ScienceAsia 49 (2023): **403–410**

In vitro anticancer efficacy of silibinin-loaded PLGA nanofibers against A549 non-small-cell lung cancer cells

Qiong Wu, Shiguang Xu, Wei Xu, Hao Meng*

Department of Thoracic Surgery, General Hospital of Northern Theater Command, Shenyang 110011 China

*Corresponding author, e-mail: mh7713642@sina.com

Received 26 Apr 2022, Accepted 11 Dec 2022
Available online 15 May 2023

ABSTRACT: In recent years, amount of evidence suggests that silibinin (SLB), an active constituent isolated from the seeds of Silybum marianum, possesses pleiotropic anticancer effects in different cancers. In this study, poly (lactic-co-glycolic acid) (PLGA) polymer was used to fabricate SLB containing nanofibers (NFs) by the electrospinning method. The NFs were characterized by their unique morphological features, degradation rate, and drug release profile. The cytotoxic effects, production of intracellular reactive oxygen species (ROS), and the gene expression of apoptotic proteins were investigated in A549 human lung adenocarcinoma cells and normal human lung epithelial cell line (BEAS-2B cells) treated with free SLB and SLB-loaded PLGA NFs. The results indicated that both free SLB and SLB-loaded NFs had no effect on BEAS-2B cells, but were cytotoxic against A549 cells, increasing intracellular ROS levels in cancer cells. In addition, both agents induced the gene expression of apoptotic proteins, and the SLB-loaded NFs acted more efficiently than the free SLB. With further study, hence, the SLB-loaded NFs could be potentially used as an anti-cancer agent against human lung adenocarcinoma.

KEYWORDS: silibinin, electrospinning, nanofiber, PLGA, lung cancer

INTRODUCTION

Lung cancer is one of the most commonly diagnosed cancers worldwide, making up almost 25% of all cancer deaths [1, 2]. 5-year survival rate for lung cancer is as low as 18%. The survival rate is improved to 54% with non-metastatic disease, making feasible the surgical removal of the primary mass [3]. Still, the early-stage lung cancer survival is considerably poor in comparison to surgical outcomes for early-stage breast and prostate cancers where 5-year survival rates are higher than 90% [4]. Lung cancer compromises the lung function. Therefore, massive local excision of the tumor, i.e. lobectomy, exacerbates the already limited pulmonary function. While on the other hand, wedge resection preserves lung tissue, the cancer recurrence rate is increased up to two-fold caused by the remaining tumor cells at the resection site [5]. Since 2-year survival diminishes to as low as 20%, further surgical resection is not warranted; and chemotherapy and radiotherapy are largely palliative [6]. Therefore, devising novel measures to efficiently control the local recurrence rate of lung cancer is highly needed.

Localized implantable devices are novel drug delivery systems that guarantee the high concentration of the drugs at the tumor site with the advantage of low systemic side effects by circumventing the systemic circulation [7, 8]. Polymeric electrospun nanofibers (NFs) are localized implantable devices known for their nano-scale sizes, adjustable surface morphology, similar structure to the extracellular matrix (ECM), favourable surface area to volume ratio, and higher drug-loading volume with the capacity to co-deliver various therapeutic agents [9, 10]. Electrospinning is an efficient technique for constructing NFs from diverse substances like composites and ceramics [11, 12]. The therapeutic agents are incorporated into the NFs through various electrospinning methods like blend, coaxial, and emulsion electrospinning [13, 14].

Silibinin (SLB), a flavonoid compound isolated from *Silybum marianum* with anti-proliferative and apoptotic effects both *in vitro* and *in vivo*, has been implemented as a chemopreventive agent [15, 16]. SLB has a negligible effect on non-cancerous cells, and phase I studies on humans have revealed that SLB is well tolerated in patients with prostate cancer [17]. SLB exerts antitumor effects by various mechanisms including mitochondrial outer membrane permeabilisation, inhibition of apoptosis, cell proliferation, angiogenesis, and metastasis, induction of cell cycle arrest, and increasing the generation of intracellular reactive oxygen species (ROS) [18, 19]. SLB has anti-cancer effects against various cancers including prostate [20], colorectal [21], and breast cancers [22]. Moreover, its activity against lung cancer is thoroughly investigated and well documented [23].

In the present study, we examined the practicability of SLB loading onto poly (D,L-lactide-*co*-glycolide) (PLGA) NFs by blend electrospinning technique, aiming to utilize it as an implantable drug for the treatment of lung cancer and for the prevention of disease recurrence. Since PLGAs are highly biodegradable and biocompatible NFs for the delivery of anti-cancer agents [24], PLGA NFs opted for the nanoencapsulation purposes. To investigate comparatively the *in vitro* cytotoxic effects, the degree of ROS production, as well as the apoptosis induction, A549 human lung adenocarcinoma cells were treated with both free SLB

and SLB-loaded PLGA NFs.

MATERIALS AND METHODS

Materials

The A549 human lung adenocarcinoma cells and human normal lung epithelial cells (BEAS-2B) were obtained from the Pasteur Institute of Iran. Fetal Bovine Serum (FBS) and RPMI1640 were provided from Gibco, Invitrogen, UK. Penicillin G, streptomycin, silibilin, poly(D,Llactide-*co*-glycolide) (PLGA, Mw 38–54 kDa, lactide:glycolide = 50:50), dichloromethane, methanol, dimethyl sulfoxide (DMSO), 3(4,5-dimethyl thiazol-2-yl)2, 5-diphenyl-tetrazolium bromide (MTT), and 2′,7′-dichlorofluorescein diacetate (DCFDA) were obtained from Sigma-Aldrich (St Louis, Missouri, USA). TRIzol reagent was obtained from Invitrogen, Carlsbad, CA, USA. Revert Aid First-strand cDNA Synthesis Kit was obtained from Fermentas, St Leon-Rot, Germany. SYBR Green Master Mix was purchased from Takara, Kusatsu, Japan.

Electrospinning

A mixture of dichloromethane and methanol (4:1, v/v) at a concentration of 20% (w/v) was implemented to dissolve PLGA for the preparation of an electrospinnable solution. To gain 20% (wt/wt %) SLB-PLGA NFs, 1 g of SLB was added into 5 g of PLGA solution and stirred magnetically overnight at 25 °C. Then, the solution was loaded into a 10 ml plastic syringe with a blunted 22-gauge needle and introduced into the electrospinning system (FNM Ltd., Iran). The electrospinning was performed at a voltage of 22 kV with a flow rate of 1.0 ml/h, and a needle-to-collector distance of 200 mm. Ultimately, the manufactured electrospun NFs were collected on a foil-coated rotating collector and subsequently dried overnight under a vacuum oven to remove the residual solvents.

Fiber characterization

Field emission scanning electron microscopy (FE-SEM) (MIRA3 TESCAN, Czech) with an accelerating voltage of 10 kV was utilized to evaluate the morphological features of the NFs. The mean diameter of the mats was quantitated by the image analysis software (Image J, National Institutes of Health, Bethesda, VA) through measuring the diameter of 100 randomly selected fibers from the FE-SEM photographs. The crystallinity of SLB-loaded PLGA NFs were examined by X-ray diffraction (Bruker AXS model D8Advance diffractometer using CuKα radiation (λ = 1.542 Å) with the Bragg angle ranging from 10° to 70°. To examine the fiber degradation rate, 10 mg of the NFs were incubated with 2 ml of phosphate buffer solution (PBS, pH 7.4) at 37 °C; and the samples were obtained, vacuum-dried for 24 h, and weighed at different times. To obtain the degradation rate of the electrospun NFs, the weight of the samples was plotted against time.

In vitro drug release profile

The SLB release pattern from the NFs was calculated in PBS buffer at 37 °C and the normal pH of extracellular fluid (pH 7.4) and the acidic environment around tumor cells (pH∼5.5). 10 mg of dried SLB-loaded PLGA NFs were put into 1 ml PBS under shaking at 60 rpm and 37 °C. At established times, the 1 ml PBS was replaced with 1 ml fresh PBS. Lambda 950 Visible-UV spectrophotometer (PerkinElmer Fremont, CA) was utilized to calculate the amount of SLB in the collected PBS via a calibration curve at the wavelength that SLB exhibits the maximum absorbance (237 nm). The accumulative discharge of SLB from the PLGA fibers was calculated as a function of incubation time.

In vitro cytotoxicity assay

The cytotoxicity of free SLB and SLB-loaded PLGA NFs against A549 non-small cell lung cancer cells was evaluated using the MTT colorimetric assay. In summary, a density of 100 cell/cm^2 was added in 24-well plates and incubated at 37 °C overnight for attachment of the NFs. Then, the cells in 1 ml media were treated with 10 mM and 20 mM of free SLB as well as the SLB-PLGA NFs in which the amount of drug was determined to be equal with the applied free drug concentrations, and incubated at 37 °C in 5% CO_2 for 48 h. Next, the media was discarded and the cells were incubated with 100 µl of MTT solution at 37 °C for 4 h. Afterward, the solution was removed, and 200 µl DMSO was added to the wells to dissolve formazan crystals. Finally, 100 µl of each sample was added to each well of the 96-well plate, and absorbance at 570 nm was determined using ELISA reader (Dynex MRX). The relative viability of the cells was measured by OD test/OD control × 100%, and the average value from three measurements was obtained.

Reactive oxygen species (ROS) determination

Intracellular ROS levels were quantitated via the peroxide-dependent oxidation of the cell-permeable fluorogenic probe 2′,7′ dichlorofluorescein diacetate (DCFDA) to the highly fluorescent 2′,7′-dichlorofluorescein (DCF). The A549 lung cancer cells were carried into black 96 well plates at a density of 104 cell/cm^2 and incubated for 24 h. Next, the cells were washed with PBS, and 20 µM of DCFDA was added to each well. After penetrating into the cells, DCFDA was hydrolyzed to the cell impermeable DCF. Then, cells were incubated for 45 min at 37 °C, the supernatant was removed, and the cells were exposed to free SLB and SLB-loaded PLGA NFs in PBS for 0.5–4 h. The generation of ROS in response to free SLB and SLB-loaded PLGA NFs were measured by quantitating the oxidation of DCFDA to the fluorescent DCF via a Synergy HT fluorescent plate reader at excitation/emission wavelength = 480/530 nm.

Real-time quantitative PCR

The *in vitro* capability of the free SLB and the SLB-loaded PLGA NFs to alter the mRNA levels of apoptotic genes (Bax, Bcl-2, caspase-3, and caspase-9) in A549 lung cancer cells were assayed by real-time quantitative PCR (qRT-PCR). The cells were exposed to free SLB and SLB-loaded PLGA NFs for 48 h. Then, the total RNA of the cells was extracted using the TRIzol reagent. The quality and quantity of the extracted RNA were assessed by electrophoresis on 1.5% agarose and OD260/280 ratio measurements via UV-Vis spectrophotometry (NanoDrop, Thermo Fisher Scientific Inc, USA), respectively. Equal amounts of RNA from individual samples were used to generate cDNA by the use of Revert Aid First-strand cDNA Synthesis Kit. Next, specific primers (Takapou Zist Co., Iran) and SYBR Green Master Mix were utilized to amplify the synthesized cDNAs via qRT-PCR. The sequence of qRT-PCR reactions in a Rotor-Gene™ 6000 system (Corbett Research, Australia) was as follows: initial denaturation at 95 °C for 10 min; then cycles of denaturation at 95 °C for 15 s, annealing at 60 °C for 30 s, and extension at 72 °C for 30 s. Finally, amplicons were analyzed by melting curve analysis of 70 °C–95 °C. To measure the relative gene fold changes, the comparative Ct method ($2^{-\Delta\Delta CT}$) was adopted, and the validation of the expression of the target genes was normalized to the housekeeping gene Glyceraldehyde 3-phosphate dehydrogenase (GAPDH).

Statistical analysis

All tests were performed in triplicate and data were expressed as the mean ± standard deviation (SD). Statistically, differences between groups were measured by applying a one-way ANOVA test through GraphPad Prism 7.01. A value of $p < 0.05$ was considered statistically significant.

RESULTS

Fiber characterization

Blend electrospinning was performed to generate PLGA NFs containing SLB. Fig. 1 shows FE-SEM micrographs of the neat PLGA and SLB-loaded PLGA NFs. Both types could be transformed into a bead-free, smooth surface, randomly-oriented electrospun NFs with a well-interconnected porosity which can augment the tumor cell trapping and prevent cell migration and metastasis.

The mean diameters of the neat PLGA NFs and the SLB-loaded PLGA NFs were 330 ± 65 nm and 370 ± 51 nm, respectively. Loading SLB into PLGA NFs slightly increases the fiber diameter. To examine the crystallization characteristics of SLB in the PLGA NFs, XRD analysis was performed. The XRD patterns of pure SLB, PLGA, and SLB-loaded PLGA NFs were demonstrated in Fig. 2. The sharp peaks of pure SLB, especially at 2θ angles, were 15°, 20°, 22°, 30°, and 42° denoting the crystalline form of pure SLB. The diffractograms of SLB-PLGA revealed the shapeless state of the polymer. In the XRD of the PLGA, low-intensity peaks across the range of 15–25 θ were noted, resembling a dome-shaped graph. It could be deduced that a relative amount of SLB existed on or close to the surface of the NFs, since internalization of the agent into the NFs stopped recrystallization of SLB as the crystal nucleation was inhibited.

In vitro degradation

Fig. 3A shows the *in vitro* matrix degradation rates of the neat PLGA and SLB-loaded PLGA NFs. During the first 3 days, no loss of NFs was detected. However, in the following days, degradation of the PLGA occurred at a relatively constant rate due to the low molecular weight of the material. The degradation rates of the neat PLGA NFs and SLB-loaded PLGA NFs were almost identical since the amount of SLB loaded onto PLGA NFs was relatively low and constituted a small portion of the total weight of the fibers.

Release profile

The cumulative SLB release from the PLGA NFs was examined at pH 7.4 and pH 6.0. As shown in Fig. 3B, SLB release had two consecutive phases: the initial rapid phase over 72 h during which almost 69% of the SLB was released and the late constant phase in which the remaining SLB was slowly discharged over a 16-day period. Furthermore, no difference was noted between the release pattern of SLB at pH = 5.5 and pH 7.4.

Cytotoxic effects

The cytotoxicity of both pure and NF-loaded SLB was examined in A549 lung cancer cells by the MTT assay (Fig. 4A). Increasing concentrations of SLB led to reduced cell viability in a dose-dependent manner. Based on these preliminary findings, the 20 mM dose of SLB was selected for further evaluation. By mass molarity calculation and by measuring the amount of SLB in a fixed weight of NFs using UV-vis spectroscopy at λ_{max} of SLB (237 nm), 120 mg of NFs containing 2.5 mg of SLB in 1 ml media equal to 20 mM of free SLB was chosen for MTT assay. As shown in Fig. 4B, neat NFs, free SLB, and SLB-NFs had no significant effect on the viability of normal human lung epithelial cell line (BEAS-2B cells). While SLB significantly reduced the viability of A549 lung cancer cells, the SLB-loaded NFs further diminished the viability; and the difference between free SLB and SLB-loaded NFs was statistically significant (Fig. 4C).

Generation of ROS

The ROS generation in A549 lung cancer cells treated with free SLB and SLB-loaded NFs was examined at different time intervals in tissue culture polystyrene (TCP) control group and unloaded neat NFs group.

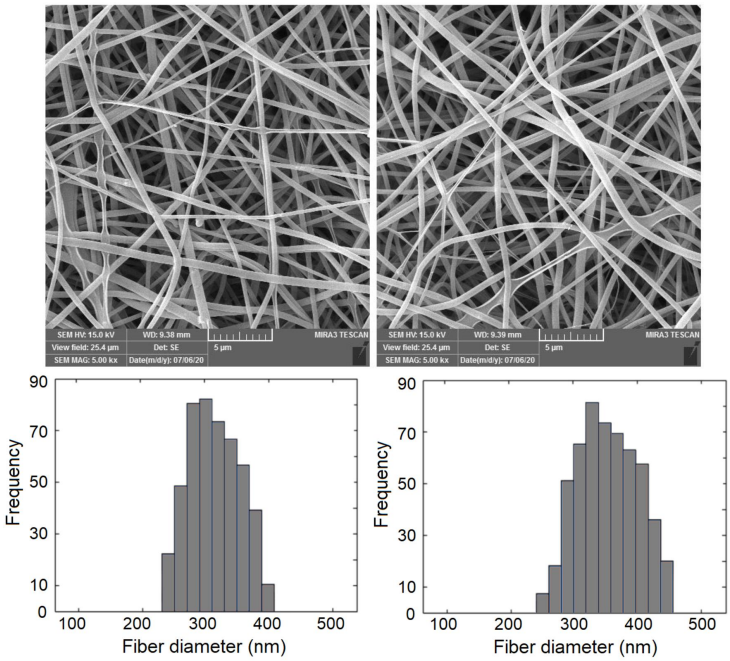

Fig. 1 FE-SEM micrograph and corresponding diameter distribution for neat PLGA NFs (left) and SLB-loaded PLGA NFs (right).

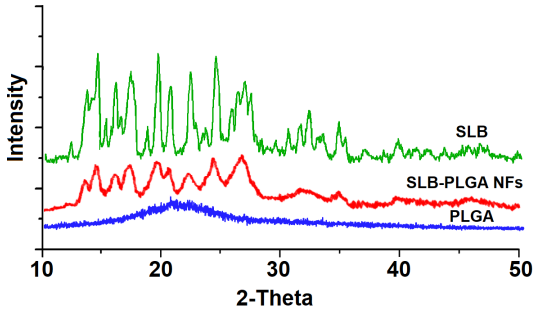

Fig. 2 XRD patterns of pure SLB, PLGA NFs, and SLB-loaded PLGA NFs.

However, SLB-loaded NFs significantly and time-dependently elevated the intracellular levels of ROS (Fig. 5). As noted in Fig. 5, free SLB was also capable of increasing the intracellular levels of ROS; however, SLB-loaded NFs acted more efficiently compared with free SLB.

Apoptosis related gene expression

The gene expression of proteins involved in apoptosis was investigated (Fig. 6). The results revealed that both free SLB and SLB-loaded NFs increased the gene expression of apoptotic proteins Bax, caspase 3, and caspase 9; and meanwhile, both agents reduced the gene expression of anti-apoptotic proteins Bcl-2 and hTERT. Generally, SLB-loaded NFs performed more efficiently than free SLB. It should be underlined that the expression of all above-mentioned genes remained unchanged in TCP control group and neat unloaded NFs group.

DISCUSSION

The findings of the present investigation demonstrated that SLB-loaded NFs had cytotoxic effects on the A549 lung cancer cells and induced the apoptotic genes. However, further in-depth studies are essential to evaluate the *in vivo* efficiency of the compound, and to elucidate the related molecular mechanisms.

As underlined in the results section, the release of SLB from the PLGA NFs had a biphasic pattern; an initial rapid phase and a late gradual phase. The initial rapid release could be the consequence of the diffusion of SLB located on the surfaces of the NFs; however, the sustained discharge of SLB could be ascribed to the slow degradation of PLGA NFs [25]. This was supported by the finding that the weight of the PLGA NFs remained relatively constant in the initial phase and then began to decrease gradually. Mirzaeei et al incorporated amoxicillin and metronidazole on PLGA electrospun NFs and found that about 80% of the agents were released over the initial 90 h, followed by a gradual liberation of the agents over the next 200 h [26]. Likewise, releases of artemisinin from the polycaprolactone/collagen NFs demonstrated a similar biphasic release pattern [27, 28]. Moreover, the release pattern of SLB did not change in pH 5.5 and

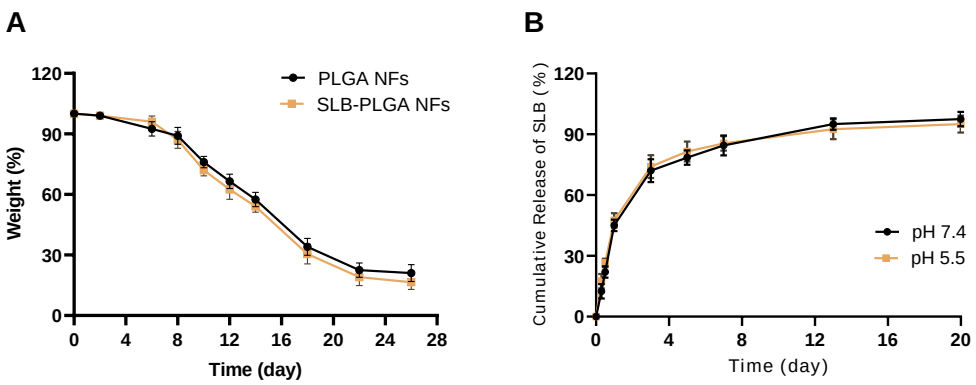

Fig. 3 *In vitro* degradation patterns of PLGA NFs and SLB-loaded PLGA NFs as a function of incubation time in PBS with pH 7.4 (A), and the drug release profile of SLB from SLB-loaded PLGA NFs in PBS at pH 7.4 and pH 5.5 (B). The data are presented as mean ± SD ($n = 3$).

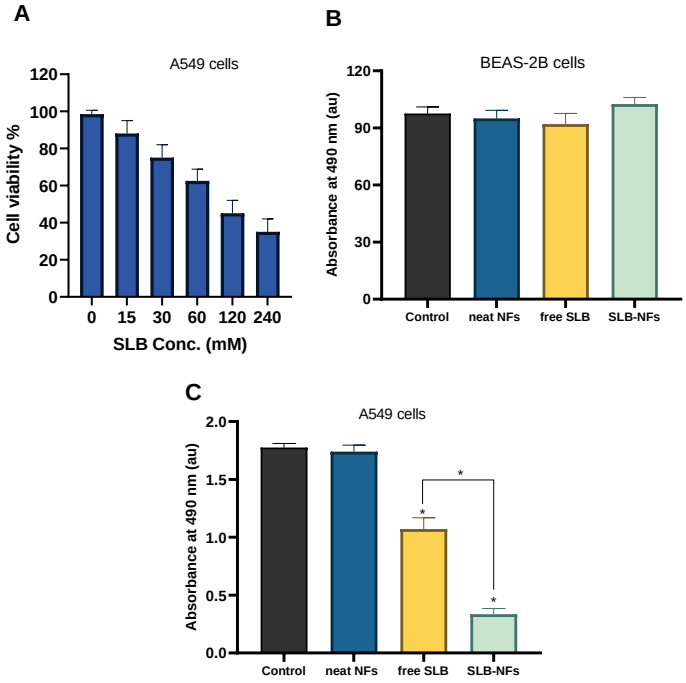

Fig. 4 *In vitro* cytotoxicity of different concentrations of free SLB to determine the IC_{50} value on A549 lung cancer cells (A), the cytotoxicity of free SLB and SLB-loaded PLGA NFs on the BEAS-2B cells after 48 h via MTT assay (B), and the A549 cells (C). * indicates a significant difference at $p < 0.05$. Values are expressed as mean ± SD of three parallel measurements.

pH 7.4; this is important because local hypoxemia acidifies the environment around the tumors, thereby altering the kinetics of the released drug [29]. We found that SLB-loaded NFs were more cytotoxic to A549 lung cancer cells in comparison to the free SLB. This is attributed to the fact that the free drug is susceptible to degradation and is rapidly metabolized and inactivated by the cells. However, a substantial amount of drug loaded on the PLGA nano scaffold is rapidly diffused out, exerting its therapeutic effects, followed by the second stage drug release owing to the gradual degradation of PLGA NFs and sustained release of the drug, rendering the intact therapeutic substance available for much longer periods which enhances its therapeutic efficiency [30].

Cancer cells have higher levels of ROS compared

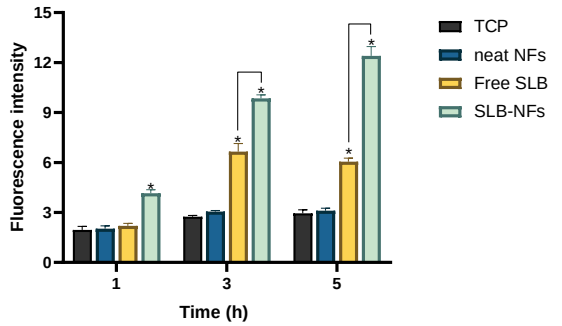

Fig. 5 ROS levels in A549 lung cancer cells treated with SLB and SLB-loaded PLGA NFs in different time points. $^{*}p < 0.05$ versus control group. Results are mean ± SD ($n = 3$). TCP, tissue culture polystyrene (control group without drug/fiber); neat NFs, drug-unloaded nanofibers; Free SLB, free silibinin; SLB-NFs, silibinin-nanofibers.

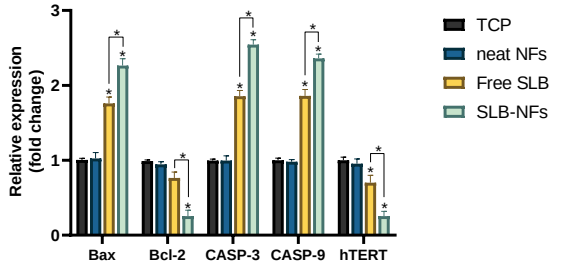

Fig. 6 Relative gene expression levels of Bax, Bcl-2, caspase-3, caspase-9, and hTERT in A549 lung cancer cells treated with SLB and SLB-loaded PLGA NFs after 48-h incubation time. $^{*}p < 0.05$ versus control was considered significant. Results are mean ± SD ($n = 3$). TCP, tissue culture polystyrene (control group without drug/fiber); neat NFs, drug-unloaded nanofibers; Free SLB, free silibinin; SLB-NFs, silibinin-nanofibers.

with normal cells due to increased cell metabolism; however, the redox balance is maintained in cancer cells caused by elevated antioxidant capacity. It is now known that most chemotherapeutic drugs exert oxidative stress by induction of ROS generation or by inhibition of antioxidant pathways. Therefore, redox balance is disturbed in cancer cells and initiates ROS-mediated cell damage in tumor cells [31]. In the present work, it was shown that SLB elevated intracellular levels of ROS in A549 cells. In line with these findings, Kim et al [32] demonstrated that SLB increased the production of ROS in breast cancer cells by downregulating the notch-1/ERK/Akt signaling pathways and consequently inducing cell death.

Apoptosis is a process of programmed cell death mediated by a cascade of consecutive proteins especially caspases, that are activated upon exposure to ionizing radiation and chemotherapeutic agents [33, 34]. It had been shown that SLB induced apoptosis by inducing the cleavage of caspase 3 and poly (ADO-ribose) polymerase 1 (PARP-1), triggering cell death in glioblastoma cell lines [35]. Moreover, it was demonstrated that the treatment of pancreatic cancer cells (SW1990) with SLB at the concentration of 200 μM increased the population of apoptotic cells to 27.69%, while the apoptotic rate in the normal pancreatic cells was only 8.84% [36]. The Bcl-2 family, the principal regulators of apoptosis, consists of proteins that either induce or oppose apoptosis. The increased ratio of pro-apoptotic Bax to anti-apoptotic Bcl-2 and Bcl-xL proteins triggers apoptosis and leads to increased permeability of the outer membranes of the mitochondria [37]. Furthermore, human telomerase reverse transcriptase (hTERT) is the catalytic subunit of telomerase holoenzyme, increased expression of which augments telomerase activity in cancer cells that opposes apoptosis and maintains cell longevity [38, 39]. In the present study, we demonstrated that SLB was capable of increasing the gene expression of apoptotic proteins bax, caspase 3, and caspase 9; and reducing the gene expression of anti-apoptotic proteins bcl-2 and hTERT in A549 cells. These findings were in line with the results obtained by Amirsaadat et al [18] that showed SLB-loaded nanoparticles downregulated the gene expression of hTERT in A549 lung cancer cells.

CONCLUSION

To obtain SLB loaded PLGA NFs, we utilized the blend electrospinning technique. Nearly 70% of SLB was released initially during the first 3 days, followed by a sustained SLB discharge owing to the gradual degradation of the nanofibrous scaffold. It was found that SLB-loaded NFs were more effective in terms of cytotoxic properties against A549 lung cancer cells compared with free SLB due to constant release and availability of the drug during the treatment period. Moreover, SLB-loaded NFs significantly increased the intracellular ROS generation, a determining factor in inducing cell apoptosis. This was supported by the finding that the gene expression of pro-apoptotic genes, including bax, caspase 3, and caspase 9, were upregulated; and simultaneously, the gene expression of anti-apoptotic genes, including bcl-2 and hTERT, were downregulated in the A549 lung cancer cells. In conclusion, the SLB-loaded PLGA NFs could potentially be used as the implantable drug delivery system for the prevention of lung cancer re-emergence after surgical resection.

Acknowledgements: This work was supported by grants from the Department of Thoracic Surgery, General Hospital of Northern Theater Command, Shenyang, China.

REFERENCES

1. Sheervalilou R, Shahraki O, Hasanifard L, Shirvaliloo M, Mehranfar S, Lotfi H, Pilehvar-Soltanahmadi Y, Bahmanpour Z, et al (2020) Electrochemical nano-biosensors as novel approach for the detection of lung cancer-related microRNAs. *Curr Mol Med* **20**, 13–35.
2. Sheervalilou R, Ansarin K, Fekri Aval S, Shirvaliloo S, Pilehvar-soltanahmadi Y, Mohammadian M, Zarghami N (2016) An update on sputum Micro RNAs in lung cancer diagnosis. *Diagn Cytopathol* **44**, 442–449.
3. Mellatyar H, Talaei S, Pilehvar-Soltanahmadi Y, Dadashpour M, Barzegar A, Akbarzadeh A, Zarghami N (2018) 17-DMAG-loaded nanofibrous scaffold for effective growth inhibition of lung cancer cells through targeting HSP90 gene expression. *Biomed Pharmacother* **105**, 1026–1032.
4. Kaplan JA, Liu R, Freedman JD, Padera R, Schwartz J, Colson YL, Grinstaff MW (2016) Prevention of lung cancer recurrence using cisplatin-loaded superhydrophobic nanofiber meshes. *Biomaterials* **76**, 273–281.
5. Kraev A, Rassias D, Vetto J, Torosoff M, Ravichandran P, Clement C, Kadri A, Ilves R (2007) Wedge resection vs lobectomy: 10-year survival in stage I primary lung cancer. *Chest* **131**, 136–140.
6. Uramoto H, Tanaka F (2014) Recurrence after surgery in patients with NSCLC. *Transl Lung Cancer Res* **3**, 242.
7. Samadzadeh S, Babazadeh M, Zarghami N, Pilehvar-Soltanahmadi Y, Mousazadeh H (2021) An implantable smart hyperthermia nanofiber with switchable, controlled and sustained drug release: Possible application in prevention of cancer local recurrence. *Mater Sci Eng C* **118**, 111384.
8. Wei W, Zarghami N, Abasi M, Ertas YN, Pilehvar Y (2022) Implantable magnetic nanofibers with ON–OFF switchable release of curcumin for possible local hyperthermic chemotherapy of melanoma. *J Biomed Mater Res A* **110**, 851–860.
9. Nejati-Koshki K, Pilehvar-Soltanahmadi Y, Alizadeh E, Ebrahimi-Kalan A, Mortazavi Y, Zarghami N (2017) Development of Emu oil-loaded PCL/collagen bioactive nanofibers for proliferation and stemness preservation of human adipose-derived stem cells: possible application in regenerative medicine. *Drug Dev Ind Pharm* **43**, 1978–1988.
10. Zamani R, Aval SF, Pilehvar-Soltanahmadi Y, Nejati-Koshki K, Zarghami N (2018) Recent advances in cell electrospining of natural and synthetic nanofibers for regenerative medicine. *Drug Res (Stuttg)* **68**, 425–435.
11. Talaei S, Mellatyar H, Pilehvar-Soltanahmadi Y, Asadi A, Akbarzadeh A, Zarghami N (2019) 17-Allylamino-17-demethoxygeldanamycin loaded PCL/PEG nanofibrous scaffold for effective growth inhibition of T47D breast cancer cells. *J Drug Deliv Sci Tech* **49**, 162–168.
12. Sadeghi-Soureh S, Jafari R, Gholikhani-Darbroud R, Pilehvar-Soltanahmadi Y (2020) Potential of Chrysin-loaded PCL/gelatin nanofibers for modulation of macrophage functional polarity towards anti-inflammatory/pro-regenerative phenotype. *J Drug Deliv Sci Tech* **58**, 101802.
13. Zamani R, Pilehvar-Soltanahmadi Y, Alizadeh E, Zarghami N (2018) Macrophage repolarization using emu oil-based electrospun nanofibers: possible application in regenerative medicine. *Artif Cells Nanomed Biotechnol* **46**, 1258–1265.
14. Pourpirali R, Mahmoudnezhad A, Oroojalian F, Zarghami N, Pilehvar Y (2021) Prolonged proliferation and delayed senescence of the adipose-derived stem cells grown on the electrospun composite nanofiber co-encapsulated with TiO_2 nanoparticles and metformin-loaded mesoporous silica nanoparticles. *Int J Pharm* **604**, 120733.
15. Chatran M, Pilehvar-Soltanahmadi Y, Dadashpour M, Faramarzi L, Rasouli S, Jafari-Gharabaghlou D, Asbaghi N, Zarghami N (2018) Synergistic anti-proliferative effects of metformin and silibinin combination on T47D breast cancer cells via hTERT and cyclin D1 inhibition. *Drug Res (Stuttg)* **68**, 710–716.
16. Maasomi ZJ, Soltanahmadi YP, Dadashpour M, Alipour S, Abolhasani S, Zarghami N (2017) Synergistic anticancer effects of silibinin and chrysin in T47D breast cancer cells. *Asian Pac J Cancer Prev* **18**, 1283.
17. Flaig TW, Glodé M, Gustafson D, van Bokhoven A, Tao Y, Wilson S, Su LJ, Li Y, et al (2010) A study of high-dose oral silybin-phytosome followed by prostatectomy in patients with localized prostate cancer. *Prostate* **70**, 848–855.
18. Amirsaadat S, Pilehvar-Soltanahmadi Y, Zarghami F, Alipour S, Ebrahimnezhad Z, Zarghami N (2017) Silibinin-loaded magnetic nanoparticles inhibit hTERT gene expression and proliferation of lung cancer cells. *Artif Cells Nanomed Biotechnol* **45**, 1649–1656.
19. Alibakhshi A, Ranjbari J, Pilehvar-Soltanahmadi Y, Nasiri M, Mollazade M, Zarghami N (2016) An update on phytochemicals in molecular target therapy of cancer: potential inhibitory effect on telomerase activity. *Curr Med Chem* **23**, 2380–2393.
20. Wu K-j, Zeng J, Zhu G-d, Zhang L-l, Zhang D, Li L, Fan J-h, Wang X-y, et al (2009) Silibinin inhibits prostate cancer invasion, motility and migration by suppressing vimentin and MMP-2 expression. *Acta Pharmacologica Sinica* **30**, 1162–1168.
21. Raina K, Kumar S, Dhar D, Agarwal R (2016) Silibinin and colorectal cancer chemoprevention: a comprehensive review on mechanisms and efficacy. *J Biomed Res* **30**, 452.
22. Binienda A, Ziolkowska S, Pluciennik E (2020) The anticancer properties of silibinin: its molecular mechanism and therapeutic effect in breast cancer. *Curr Med Chem Anticancer Agents* **20**, 1787–1796.
23. Verdura S, CuyÃăs E, Ruiz-Torres V, Micol V, Joven J, Bosch-Barrera J, Menendez JA (2021) Lung cancer management with silibinin: a historical and translational perspective. *Pharmaceuticals* **14**, 559.
24. Firouzi-Amandi A, Dadashpour M, Nouri M, Zarghami N, Serati-Nouri H, Jafari-Gharabaghlou D, Karzar BH, Mellatyar H, et al (2018) Chrysin-nanoencapsulated PLGA-PEG for macrophage repolarization: Possible application in tissue regeneration. *Biomed Pharmacother* **105**, 773–780.
25. Zhang L, Wang Z, Xiao Y, Liu P, Wang S, Zhao Y, Shen M, Shi X (2018) Electrospun PEGylated PLGA nanofibers for drug encapsulation and release. *Mater Sci Eng C* **91**, 255–262.
26. Mirzaeei S, Mansurian M, Asare-Addo K, Nokhodchi A (2021) Metronidazole-and amoxicillin-loaded PLGA and PCL nanofibers as potential drug delivery systems

for the treatment of periodontitis: *in vitro* and *in vivo* evaluations. *Biomedicines* **9**, 975.
27. Ahmadi S, Pilehvar Y, Zarghami N, Abri A (2021) Efficient osteoblastic differentiation of human adipose-derived stem cells on TiO_2 nanoparticles and metformin co-embedded electrospun composite nanofibers. *J Drug Deliv Sci Technol* **66**, 102798.
28. Serati-Nouri H, Mahmoudnezhad A, Bayrami M, Sanajou D, Tozihi M, Roshangar L, Pilehvar Y, Zarghami N (2021) Sustained delivery efficiency of curcumin through ZSM-5 nanozeolites/electrospun nanofibers for counteracting senescence of human adipose-derived stem cells. *J Drug Deliv Sci Tech* **66**, 102902.
29. Zhang X, Lu Y, Jia D, Qiu W, Ma X, Zhang X, Xu Z, Wen F (2021) Acidic microenvironment responsive polymeric MOF-based nanoparticles induce immunogenic cell death for combined cancer therapy. *J Nanobiotechnol* **19**, 455.
30. Rasouli S, Montazeri M, Mashayekhi S, Sadeghi-Soureh S, Dadashpour M, Mousazadeh H, Nobakht A, Zarghami N, et al (2020) Synergistic anticancer effects of electrospun nanofiber-mediated codelivery of Curcumin and Chrysin: Possible application in prevention of breast cancer local recurrence. *J Drug Deliv Sci Tech* **55**, 101402.
31. Yang H, Villani RM, Wang H, Simpson MJ, Roberts MS, Tang M, Liang X (2018) The role of cellular reactive oxygen species in cancer chemotherapy. *J Exp Clin Cancer Res* **37**, 266.
32. Kim TH, Woo JS, Kim YK, Kim KH (2014) Silibinin induces cell death through reactive oxygen species-dependent downregulation of notch-1/ERK/Akt signaling in human breast cancer cells. *J Pharmacol Exp Ther* **349**, 268–278.
33. Montazeri M, Pilehvar-Soltanahmadi Y, Mohaghegh M, Panahi A, Khodi S, Zarghami N, Sadeghizadeh M (2017) Antiproliferative and apoptotic effect of dendrosomal curcumin nanoformulation in P53 mutant and wide-type cancer cell lines. *Curr Med Chem Anticancer Agents* **17**, 662–673.
34. Zhang M, Zhao H, Lin L, Chen Z (2022) *MiR-647* inhibits proliferation and improves apoptosis in cisplatin-treated non-small cell lung cancer via down-regulating *IGF2* expression. *ScienceAsia* **48**, 705–710.
35. Bai Z-L, Tay V, Guo S-Z, Ren J, Shu M-G (2018) Silibinin induced human glioblastoma cell apoptosis concomitant with autophagy through simultaneous inhibition of mTOR and YAP. *Biomed Res Int* **2018**, 6165192.
36. Zhang X, Liu J, Zhang P, Dai L, Wu Z, Wang L, Cao M, Jiang J (2018) Silibinin induces G1 arrest, apoptosis and JNK/SAPK upregulation in SW1990 human pancreatic cancer cells. *Oncol Lett* **15**, 9868–9876.
37. Pourgholi A, Dadashpour M, Mousapour A, Amandi AF, Zarghami N (2021) Anticancer potential of silibinin loaded polymeric nanoparticles against breast cancer cells: Insight into the apoptotic genes targets. *Asian Pac J Cancer Prev* **22**, 2587.
38. Jafari-Gharabaghlou D, Pilehvar-Soltanahmadi Y, Dadashpour M, Mota A, Vafajouy-Jamshidi S, Faramarzi L, Rasouli S, Zarghami N (2018) Combination of metformin and phenformin synergistically inhibits proliferation and hTERT expression in human breast cancer cells. *Iran J Basic Med Sci* **21**, 1167.
39. Zavari-Nematabad A, Alizadeh-Ghodsi M, Hamishehkar H, Alipour E, Pilehvar-Soltanahmadi Y, Zarghami N (2017) Development of quantum-dot-encapsulated liposome-based optical nanobiosensor for detection of telomerase activity without target amplification. *Anal Bioanal Chem* **409**, 1301–1310.